

SUPPORTING INFORMATION

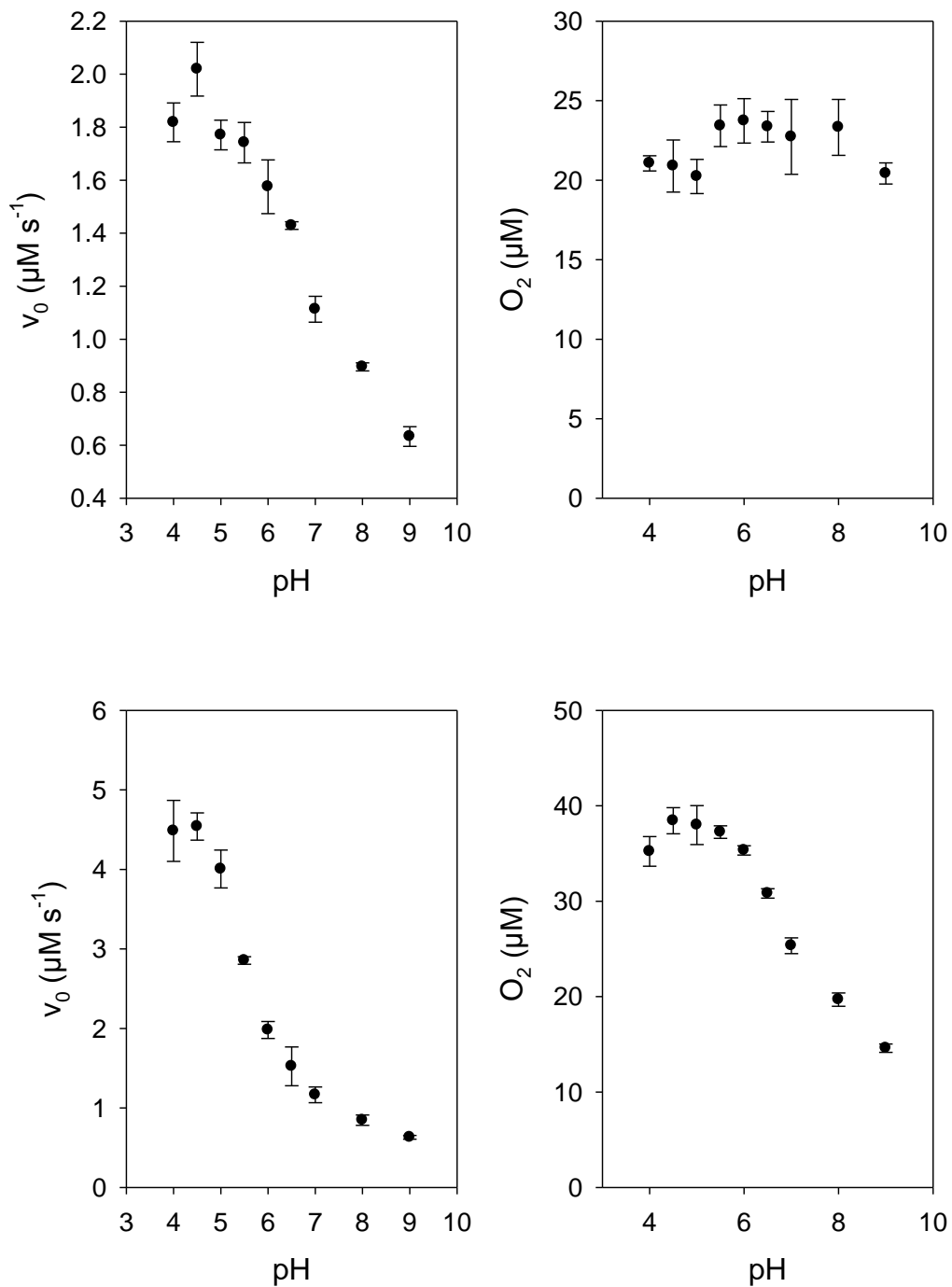
Transiently produced hypochlorite is responsible for the irreversible inhibition of chlorite dismutase

Stefan Hofbauer¹, Clemens Gruber¹, Katharina F. Pirker¹, Axel Sündermann², Irene Schaffner¹, Christa Jakopitsch¹, Chris Oostenbrink², Paul G. Furtmüller¹, Christian Obinger^{1*}

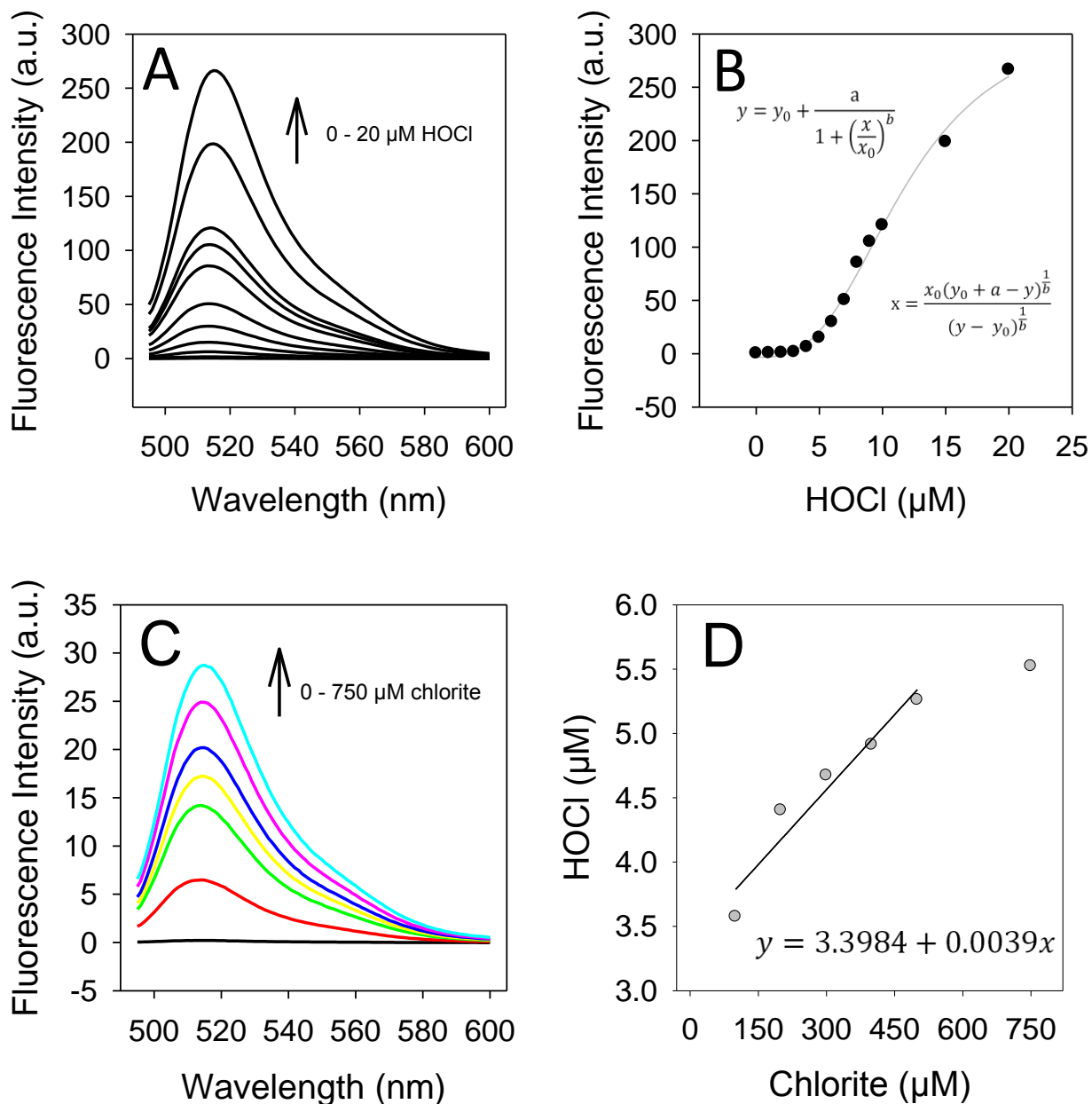
¹Department of Chemistry, Division of Biochemistry, VIBT – Vienna Institute of BioTechnology, BOKU – University of Natural Resources and Life Sciences, A-1190 Vienna, Austria

²Department of Material Sciences and Process Engineering, Institute of Molecular Modeling and Simulation, BOKU – University of Natural Resources and Life Sciences, A-1190 Vienna, Austria

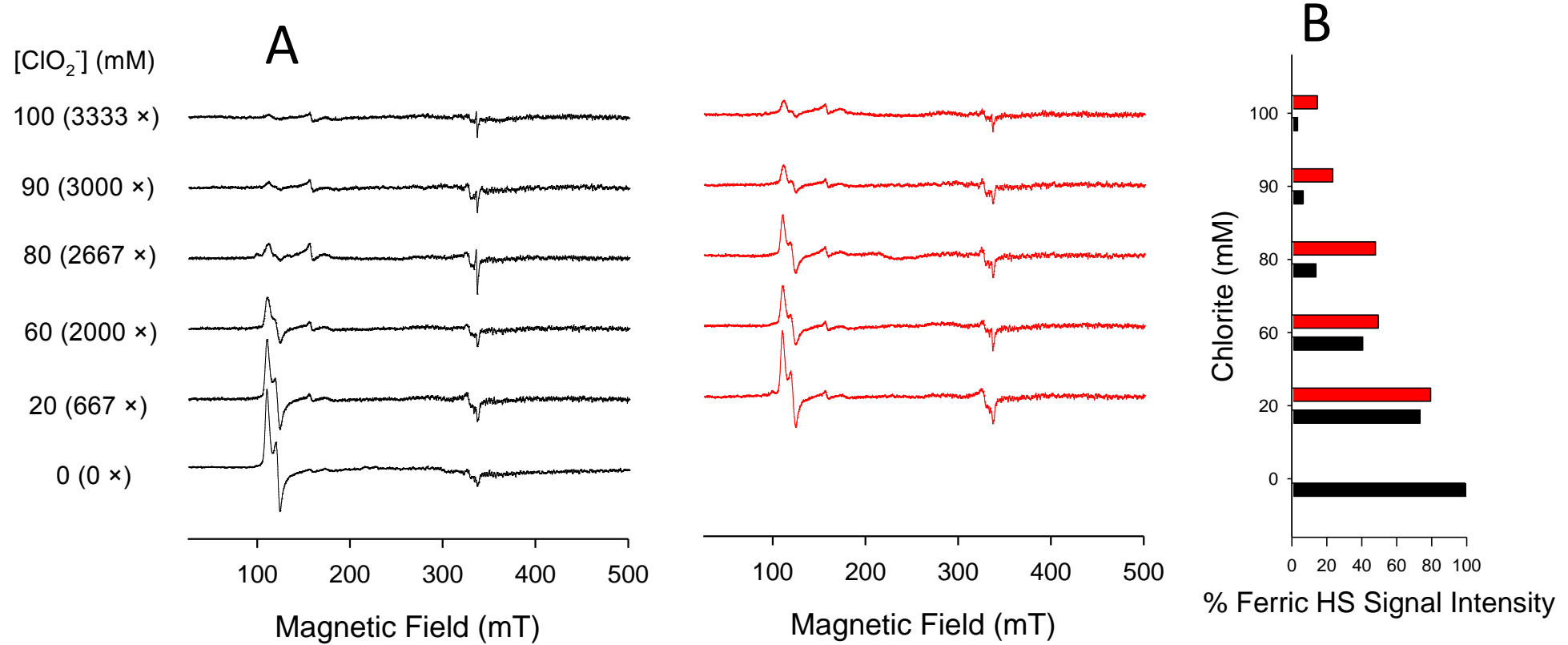
Supplemental Figure 1. pH-dependence of chlorite conversion by NdCld mutants. (A) Initial rates of production of dioxygen from 40 μ M chlorite mediated by 200 nM NdCld mutant R173A at different pH-values (50 mM citrate phosphate buffer pH 4 - 7; 50 mM phosphate buffer pH 7 - 8; 50 mM Tris/HCl buffer, pH 8 - 9). (B) Total amount of produced dioxygen in the range of pH 4 - 9. Conditions in (C), where 200 nM NdCld mutant R173K was used resembled conditions from (A); and conditions in (D) were equal to conditions in (B) using 200 nM NdCld mutant R173K.



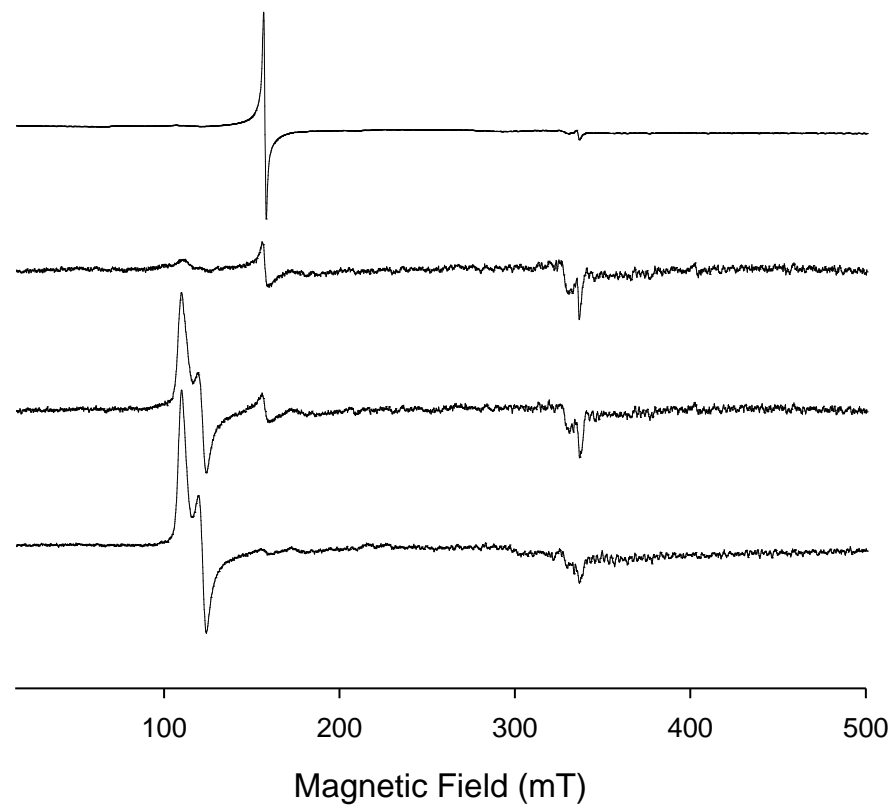
Supplemental Figure 2. Calibration curve of APF fluorescence for hypochlorite. (A) fluorescence spectra of 10 μM APF between 495 and 600 nm ($\lambda_{\text{excitation}} = 488$ nm) after reactions with 0 μM to 20 μM hypochlorite; 50 mM phosphate buffer pH 7.0. (B) Plot of fluorescence intensity versus hypochlorite concentration, showing a sigmoidal fit (logistic, 4 parameter). (C) Fluorescence spectra of 10 μM APF between 495 and 600 nm ($\lambda_{\text{excitation}} = 488$ nm) after reactions with 100 nM NdCl_d wild-type with 0 μM (black), 100 μM (red), 200 μM (green), 300 μM (yellow), 400 μM (blue), 500 μM (magenta), and 750 μM (cyan) chlorite; 50 mM phosphate buffer pH 7.0. (D) Plot of trapped HOCl concentration versus chlorite concentration, showing a linear fit between 100 and 500 μM chlorite.



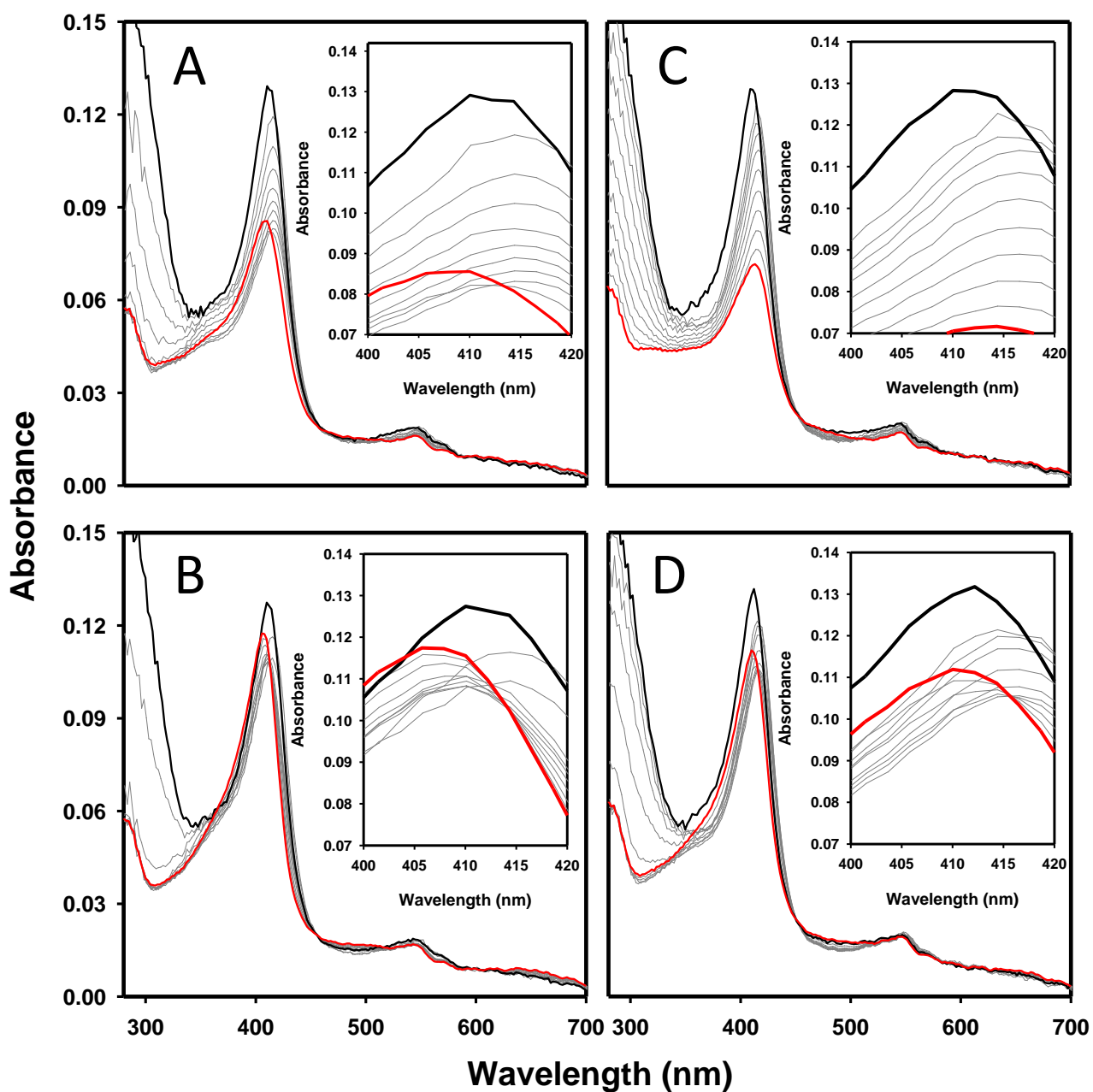
Supplemental Figure 3. (A) Electron Paramagnetic Resonance spectra of 30 μ M NdCl_d in 50 mM MES buffer, pH 5.5., in absence (black lines) and presence (red lines) of 17.5 mM methionine, after reaction with 0 mM (bottom) to 100 mM (top) chlorite. (B) Ferric high spin signal intensity of chlorite treated samples in absence (black bars) and in presence (red bars) of methionine.



Supplemental Figure 4. Influence of hypochlorite to the architecture of the heme-iron of chlorite dismutase from “*Candidatus Nitrospira defluvii*”. EPR spectra of 30 μ M wild-type NdCld treated with (bottom to top) 0 mM, 1 mM, 16 mM, and 23 mM of hypochlorite



Supplemental Figure 5. The effect of methionine on the interconversion of redox intermediates and heme bleaching. (A) Spectral changes, when 1 μ M of wild-type NdCl d was mixed with 1 mM of chlorite at pH 5.5 (50 mM citrate-phosphate buffer) in the conventional stopped-flow modus. Spectra were taken at 3 ms (black spectrum), 74 ms, 403 ms, 755 ms, 1352 ms, 2367 ms, 4090 ms, 7018 ms, and 11990 ms, respectively. The final spectrum (20000 ms) is depicted in red. Inset shows enlargement of Soret region. (B) Same reaction as in (A) but in the presence of 5 mM methionine. (C) Same reaction as in (A) but at pH 7.0 (50 mM phosphate buffer), (D) same reaction as (C) but in presence of 5 mM methionine.



Supplemental Table 1. EPR simulation parameters from individual high spin and low spin forms of NdCld at pH 5.5 and pH 7.0, eventually with chlorite and methionine (HS – high spin, LS – low spin, R – rhombicity, I – relative intensity, E/D – rhombic to axial contribution, TI – total intensity with respect to untreated protein).

	HS LS compounds*	g_x^{eff}	g_x	g_y^{eff}	g_y	g_z^{eff} g_z	E/D	R (%)	I (%)	TI (%)
NdCld pH 5.5	HS1	5.500	6.175	1.990	0.014	4.2	80	100	20	104
	HS2	5.950	5.950	1.995						
NdCld pH 5.5 + 17.5 mM methionine	HS1	5.500	6.175	1.990	0.014	4.2	49	43	13	13
	HS2	5.950	5.950	1.995					26	
NdCld pH 5.5 + 100 mM chlorite	LS1	2.980	2.250	1.875					13	
	LS2	3.150	2.250	1.800					13	
NdCld pH 5.5 + 100 mM chlorite + 17.5 mM methionine	HS1	5.625	6.225	1.990	0.013	3.7	43	14		
	HS2	5.950	5.950	1.995				57		
NdCld pH 5.5 + 100 mM chlorite + 17.5 mM methionine	HS1	5.500	6.175	1.990	0.014	4.2	50	36		
	HS2	5.950	5.950	1.995				28		
NdCld pH 5.5 + 100 mM chlorite + 17.5 mM methionine	HS3	5.250	6.375	1.975	0.025	7.0	22			
	HS1	5.500	6.175	1.990	0.014	4.2	49	100		
NdCld pH 7.0	HS2	5.950	5.950	1.995				19		
	LS1	2.980	2.250	1.875				15		
NdCld pH 7.0 + 17.5 mM methionine	LS2	3.150	2.250	1.800				16		
	HS1	5.500	6.175	1.990	0.014	4.2	32	83		
NdCld pH 7.0 + 100 mM chlorite	HS2	5.950	5.950	1.995				28		
	HS3	5.250	6.375	1.975	0.025	7.0	14			
NdCld pH 7.0 + 100 mM chlorite + 17.5 mM methionine	LS1	2.980	2.250	1.875				13		
	LS2	3.150	2.250	1.800				14		
NdCld pH 7.0 + 100 mM chlorite	HS1	5.500	6.175	1.990	0.014	4.2	18	11		
	HS2	5.950	5.950	1.995				64		
NdCld pH 7.0 + 100 mM chlorite + 17.5 mM methionine	HS3	5.450	6.225	1.990	0.017	4.8	18			
	HS1	5.500	6.175	1.990	0.014	4.2	41	42		
NdCld pH 7.0 + 100 mM chlorite + 17.5 mM methionine	HS2	5.950	5.950	1.995				23		
	HS3	5.250	6.375	1.975	0.025	7.0	36			

*minimum number of high-spin and low-spin compounds used for simulation